INTERNATIONAL JOURNAL FOR NUMERICAL AND ANALYTICAL METHODS IN GEOMECHANICS
Int. J. Numer. Anal. Meth. Geomech., 2000; **24**:579–599

Accelerated initial stiffness schemes for elastoplasticity

Scott W. Sloan[1*†‡], Daichao Sheng[2§] and Andrew J. Abbo[3¶]

[1]*Department of Civil, Surveying and Environmental Engineering, University of Newcasstle NSW 2308, Australia*
[2]*Department of Civil, Surveying and Environmental Engineering, University of Newcastle, NSW 2308, Australia*
[3]*Formation Design Systems, Fremantle, WA 6160, Australia*

SUMMARY

Iterative methods for the solution of non-linear finite element equations are generally based on variants of the Newton–Raphson method. When they are stable, full Newton–Raphson schemes usually converge rapidly but may be expensive for some types of problems (for example, when the tangent stiffness matrix is unsymmetric). Initial stiffness schemes, on the other hand, are extremely robust but may require large numbers of iterations for cases where the plastic zone is extensive. In most geomechanics applications it is generally preferable to use a tangent stiffness scheme, but there are situations in which initial stiffness schemes are very useful. These situations include problems where a nonassociated flow rule is used or where the zone of plastic yielding is highly localized.

This paper surveys the performance of several single-parameter techniques for accelerating the convergence of the initial stiffness scheme. Some simple but effective modifications to these procedures are also proposed. In particular, a modified version of Thomas' acceleration scheme is developed which has a good rate of convergence. Previously published results on the performance of various acceleration algorithms for initial stiffness iteration are rare and have been restricted to relatively simple yield criteria and simple problems. In this study, detailed numerical results are presented for the expansion of a thick cylinder, the collapse of a rigid strip footing, and the failure of a vertical cut. These analyses use the Mohr–Coulomb and Tresca yield criteria which are popular in soil mechanics. Copyright © 2000 John Wiley & Sons, Ltd.

KEY WORDS: initial stiffness method; iteration acceleration; elastoplastic

1. INTRODUCTION

A variety of iterative schemes have been proposed for the solution of non-linear finite element equations in elastoplasticity. Well-known examples of iterative schemes include the Newton–Raphson, modified Newton–Raphson, and initial stress methods. Iterative solution techniques for non-linear systems typically apply the unbalanced forces, compute the corresponding displacement increments, and then repeat this procedure until the drift from equilibrium is small.

*Correspondence to: S. W. Sloan, Department of Civil, Surveying and Environmental Engineering, University of Newcastle, NSW 2308, Australia.
†E-mail: scott.sloan@newcastle.edu.au
‡Professor
§Research Fellow
¶Software Engineer

Received 4 January 1999
Revised 17 September 1999

One major disadvantage of the Newton–Raphson family of algorithms is that the iterations may not converge, particularly when the behaviour is strongly non-linear. To overcome this, various techniques have been developed to stabilise and accelerate the convergence of Newton–Raphson schemes. These include the line search techniques of Matthies and Strang [1] and Crisfield [2,3], as well as the arc length control procedures developed by Wempner [4] and Riks [5,6]. Line search methods attempt to stabilise Newton–Raphson iterations by shrinking or expanding the current displacement increment to minimise the resulting unbalanced forces. In cases where the current search direction is poor, or where the unbalanced forces are non-smooth functions of the displacements, line searches may be of limited use. The philosophy behind arc length methods is to force the Newton–Raphson iterations to remain within the vicinity of the last converged equilibrium point. This means that the applied load must be reduced as the iterations proceed, but greatly reduces the risk of divergence for strongly non-linear problems. A detailed discussion of various arc length methods, and their practical implementation, can be found in Crisfield [7]. In a fundamental development, Simo and Taylor [8] derived the consistent tangent technique for use with the Newton–Raphson scheme. By incorporating high-order terms that are usually ignored in the standard form of the elastoplastic stiffness relations, this procedure gives a full quadratic rate of convergence. Although powerful, the method is difficult to implement for complex yield criteria because it is necessary to evaluate second derivatives of the yield function.

The choice of a reliable, efficient iteration scheme for elastoplasticity is often problem dependent. The Newton–Raphson method, while providing rapid convergence for some cases, requires the tangent stiffness matrix to be computed and factorized afresh for each iteration. This operation may be expensive for complex constitutive laws, particularly if a non-associated flow rule is employed where the governing equations are unsymmetric. The number of stiffness matrix evaluations can be reduced by using the so-called modified Newton–Raphson scheme in which the stiffness matrix is computed afresh only when the rate of convergence falls below a preset rate. Alternatively, the tangent stiffness matrix may be recomputed only once per load increment. While both of these variants slow the rate of convergence, a saving in the overall computational effort may be realised for some problems.

The initial stiffness method (also known as the initial stress or elastic stiffness method) uses the elastic stiffness matrix to compute the iterative updates for the displacements. This strategy requires the symmetric elastic stiffness matrix to be assembled and factorised only once, with all subsequent solutions being obtained by back substitution. Although each iteration is fast and the method is very stable, its rate of convergence may be slow for cases with extensive plastic yielding.

In order to improve the performance of the initial stiffness method, a variety of acceleration schemes have been proposed. In the 'alpha-constant stiffness' acceleration scheme of Nayak and Zienkiewicz [9,10], for example, each degree of freedom is accelerated individually. Although novel, this procedure has proved unreliable in practice as it tends to generate very large acceleration factors. An important modification to this approach, developed by Thomas [11], uses a single-parameter acceleration scheme based on a least-squares fit. Compared with the standard initial stiffness method, Thomas demonstrated a three-fold reduction in the number of iterations for analyses using the Drucker–Prager yield criterion. The Thomas algorithm has proven to be robust for a wide range of practical problems involving complex constitutive laws, but may be uncompetitive with full Newton algorithms once the extent of plastic yielding is significant.

The acceleration method of Chen [12] chooses the acceleration parameter so as to minimize, in a least-squares sense, the unbalanced forces at the end of each iteration. This approach is

conceptually appealing and can also be used for accelerating modified Newton–Raphson iterations. It appears to be quite successful in modelling simple constitutive laws but is unproven for complex problems involving elaborate material models.

The single-parameter acceleration scheme developed by Crisfield [3] is a simplification of his two- and three-parameter 'secant-Newton' methods and employs line searches to stabilize the iterations. Although designed for modified Newton iterations, where the stiffness is updated at the start of each load increment, this procedure can be readily adapted for use with the initial elastic stiffness. Little published data is available to assess the performance of Crisfield's one-parameter scheme, as the two- and three-parameter variants are more widely used in practice.

Finally, Liu and Lam [13] have proposed an acceleration scheme which applies a multiplier to the displacements based on the potential energy within each iteration. As their scheme does not attempt to satisfy equilibrium at the end of each iteration, its performance for large-scale problems is likely to be questionable.

In this paper, a modified version of Thomas' acceleration scheme is developed. The performance of this scheme, as well as other single-parameter acceleration schemes, is studied by considering the expansion of a thick cylinder, the collapse of a rigid strip footing, and the failure of a vertical cut. In these analyses, the material is modelled using the Mohr–Coulomb and Tresca yield criteria. For the former, the influence of a non-associated flow rule, which generates an unsymmetric tangent stiffness matrix, is investigated.

2. ACCELERATION SCHEMES

A general family of iteration schemes can be expressed in the form

$$\begin{aligned} \Delta \mathbf{U}^i &= \mathbf{K}^{-1}\mathbf{R}^{i-1} \\ \mathbf{U}^i &= \mathbf{U}^{i-1} + \Delta \mathbf{U}^i \end{aligned} \tag{1}$$

where $\mathbf{K}$ is some stiffness matrix, $\mathbf{R}^{i-1} = \mathbf{R}(\mathbf{U}^{i-1}) = \mathbf{F}_{\text{ext}} - \mathbf{F}_{\text{int}}^{i-1}$ are the residual or unbalanced forces at the start of the ith iteration, $\mathbf{F}_{\text{int}}^{i-1}$ are the internal forces at the start of the ith iteration, and $\mathbf{F}_{\text{ext}}$ are the current external forces. The internal forces at the start of the ith iteration are defined by the well-known relation

$$\mathbf{F}_{\text{int}}^{i-1} = \int \mathbf{B}^{\mathrm{T}}\boldsymbol{\sigma}^{i-1}\,\mathrm{d}V$$

in which $\mathbf{B}$ is the standard strain displacement matrix and $\boldsymbol{\sigma}$ are the stresses.

For the standard Newton–Raphson scheme, the iterative stiffness matrix $\mathbf{K}$ in Equation (1) represents the tangent stiffness matrix

$$\mathbf{K}_{\text{ep}} = \mathbf{K}_{\text{ep}}(\mathbf{U}^{i-1}) = \int \mathbf{B}^{\mathrm{T}}\mathbf{D}_{\text{ep}}\mathbf{B}\,\mathrm{dV}$$

while, for an initial stiffness iteration, it represents the elastic stiffness matrix

$$\mathbf{K}_{\text{e}} = \int \mathbf{B}^{\mathrm{T}}\mathbf{D}_{\text{e}}\mathbf{B}\,\mathrm{d}V$$

where $\mathbf{D}_{\text{e}}$ and $\mathbf{D}_{\text{ep}}$ are, respectively, the elastic and elastoplastic stress–strain matrices.

The single-parameter schemes considered here avoid the formation of the tangent stiffness matrix and attempt to accelerate the convergence rate of the initial stiffness scheme using a variety of updates. Each of these will be discussed in turn.

2.1. The Chen scheme

The single-parameter Chen [12] scheme attempts to accelerate the convergence rate of the initial stiffness scheme by scaling the iterative displacements according to

$$\mathbf{U}^i = \mathbf{U}^{i-1} + \alpha^i \Delta \mathbf{U}_e^i \tag{2}$$

where α^i is a scalar and

$$\Delta \mathbf{U}_e^i = [\mathbf{K}_e]^{-1}\{\mathbf{R}^{i-1}\} \tag{3}$$

are the displacements computed using the initial stiffness matrix.

The Chen acceleration factor α^i is chosen so as to minimize the unbalanced forces at the end of the ith iteration (i.e. at $\mathbf{U}^i$) and assumes that the local load–deformation response is approximately linear. Under this assumption, the unbalanced forces vary linearly with α according to

$$\mathbf{R}^i \approx \mathbf{R}^{i-1} + \alpha^i\{\mathbf{R}_e^i - \mathbf{R}^{i-1}\} \tag{4}$$

where

$$\mathbf{R}^i = \mathbf{R}(\mathbf{U}^i) = \mathbf{R}(\mathbf{U}^{i-1} + \alpha^i \Delta \mathbf{U}_e^i)$$

and

$$\mathbf{R}_e^i = \mathbf{R}(\mathbf{U}^{i-1} + \Delta \mathbf{U}_e^i)$$

Least-squares minimization of the unbalanced forces $\mathbf{R}^i$ requires that

$$\frac{\mathrm{d}}{\mathrm{d}\alpha^i}\{\{\mathbf{R}^i\}^{\mathrm{T}}\{\mathbf{R}^i\}\} = 0 \tag{5}$$

Substituting Equation (4) into (5) and solving for α^i gives the Chen acceleration parameter as

$$\alpha^i = -\frac{\{\mathbf{R}_e^i - \mathbf{R}^{i-1}\}^{\mathrm{T}}\{\mathbf{R}^{i-1}\}}{\{\mathbf{R}_e^i - \mathbf{R}^{i-1}\}^{\mathrm{T}}\{\mathbf{R}_e^i - \mathbf{R}^{i-1}\}} \tag{6}$$

Each iteration of this algorithm requires one backsubstitution and two unbalanced force evaluations. In a recent study, Abbo and Sloan [14] observed that the acceleration parameter calculated from (6) can sometimes be much less than 1, which often leads to failure of convergence. To avoid this problem, the Chen scheme can be modified so that it uses the initial stiffness solution for the iteration whenever α^i falls below 1, i.e.

$$\alpha^i = \max\left\{-\frac{\{\mathbf{R}_e^i - \mathbf{R}^{i-1}\}^{\mathrm{T}}\{\mathbf{R}^{i-1}\}}{\{\mathbf{R}_e^i - \mathbf{R}^{i-1}\}^{\mathrm{T}}\{\mathbf{R}_e^i - \mathbf{R}^{i-1}\}}, 1\right\} \tag{7}$$

In this paper, the modified Chen accelerator given by (7) is used instead of the original accelerator given by (6).

2.2. The Thomas scheme

The acceleration scheme of Thomas [11] is also derived by a least-squares minimization process. In this method, the displacement update is assumed to be of the same form as Equation (2) and the unbalanced forces at the end of the iteration are given as

$$\mathbf{R}^i = \mathbf{R}^{i-1} - \alpha^i \mathbf{K}_{ep} \Delta \mathbf{U}_e^i \tag{8}$$

where the term $\alpha^i \mathbf{K}_{ep} \Delta \mathbf{U}_e^i$ corresponds to the increment in the internal forces due to the displacements $\alpha^i \Delta \mathbf{U}_e^i$. Decomposing the tangent stiffness matrix into its elastic and plastic components according to

$$\mathbf{K}_{ep} = \mathbf{K}_{ep}(\mathbf{U}^{i-1}) = \mathbf{K}_e - \mathbf{K}_p(\mathbf{U}^{i-1}) = \mathbf{K}_e - \mathbf{K}_p \tag{9}$$

and combining the approximation

$$\alpha^i \mathbf{K}_p \Delta \mathbf{U}_e^i \approx \alpha^{i-1} \mathbf{K}_p \Delta \mathbf{U}_e^i$$

with Equation (3) gives

$$\mathbf{K}_e^{-1} \mathbf{R}^i \approx (1 - \alpha^i) \Delta \mathbf{U}_e^i + \Delta \mathbf{U}_p^i \tag{10}$$

where

$$\Delta \mathbf{U}_p^i = \alpha^{i-1} \mathbf{K}_e^{-1} \mathbf{K}_p \Delta \mathbf{U}_e^i \tag{11}$$

Performing a least-squares minimization on the displacements $\mathbf{K}_e^{-1} \mathbf{R}^i$ leads to the Thomas [11] accelerator

$$\alpha^i = \frac{\{\Delta \mathbf{U}_e^i\}^T \{\Delta \mathbf{U}_e^i + \Delta \mathbf{U}_p^i\}}{\{\Delta \mathbf{U}_e^i\}^T \{\Delta \mathbf{U}_e^i\}} \tag{12}$$

One method for computing the displacements $\Delta \mathbf{U}_p^i$, defined by Equation (11), is to evaluate the quantity $\mathbf{K}_p \Delta \mathbf{U}_e^i$ element by element. This multiplication, together with two backsubstitutions and one unbalanced force evaluation, comprises the bulk of the work for each iteration. A second method for computing $\Delta \mathbf{U}_p^i$, suggested by Thomas in his original paper, uses the relation

$$\Delta \mathbf{U}_p^i = \alpha^{i-1} \mathbf{K}_e^{-1} \mathbf{K}_p \Delta \mathbf{U}_e^i = \mathbf{K}_e^{-1} \int \mathbf{B}^T (\mathbf{D}_e - \mathbf{D}_{ep}) \mathbf{B} \alpha^{i-1} \Delta \mathbf{U}_e^i \, dV \tag{13}$$

In this paper we adopt the first method, but also investigate an improved form of (13) which is simpler to implement in a traditional finite element code. Rather than trying to minimize the unbalanced forces at the end of the iteration, as in the Chen scheme, the Thomas algorithm attempts to minimize the elastic displacements for the next iteration. This interpretation follows from the fact that it minimizes, in a least-squares sense, the quantity $\Delta \mathbf{U}^{i+1} = \mathbf{K}_e^{-1} \mathbf{R}^i$.

When implementing the Thomas scheme, there are in fact two choices for updating the displacements. The first choice, which is the obvious one, uses Equation (2) after α^i is found from Equation (12). In practice, extensive testing has shown that this option provides only moderate convergence acceleration and should be avoided. A much better choice, which was adopted by Thomas [11], uses the fact that the least-squares minimization of the displacements $\mathbf{K}_e^{-1} \mathbf{R}^i$ in

Equation (10) is equivalent to selecting α^i so that

$$\alpha^i \Delta \mathbf{U}_e^i \approx \Delta \mathbf{U}_e^i + \Delta \mathbf{U}_p^i$$

Hence an alternative displacement update is

$$\mathbf{U}^i = \mathbf{U}^{i-1} + \Delta \mathbf{U}_e^i + \Delta \mathbf{U}_p^i \tag{14}$$

A key feature of this option is that it only uses the acceleration factor from the previous iteration in order to compute the displacement update. In the first iteration of each load increment, the process may be started by assuming that $\alpha^0 = 1$. We will show later in the paper that Equations (12) and (14) improve the convergence of the initial stiffness method dramatically and reliably.

2.3. The modified Thomas scheme

A simple refinement to the Thomas method, which is more convenient to implement in a standard finite element code, can be derived by using Equations (3), (9) and (11) to rewrite Equation (14) as

$$\mathbf{U}^i = \mathbf{U}^{i-1} + \alpha^{i-1} \Delta \mathbf{U}_e^i + \mathbf{K}_e^{-1} \{ \mathbf{R}^{i-1} - \alpha^{i-1} \mathbf{K}_{ep} \Delta \mathbf{U}_e^i \}$$

Using the approximation

$$\mathbf{R}^{i-1} - \alpha^{i-1} \mathbf{K}_{ep} \Delta \mathbf{U}_e^i \approx \mathbf{R}(\mathbf{U}^{i-1} + \alpha^{i-1} \Delta \mathbf{U}_e^i)$$

the new update may be written as

$$\mathbf{U}^i = \mathbf{U}^{i-1} + \alpha^{i-1} \Delta \mathbf{U}_e^i + \Delta \tilde{\mathbf{U}}_e^i \tag{15}$$

where

$$\Delta \tilde{\mathbf{U}}_e^i = \mathbf{K}_e^{-1} \{ \mathbf{R}(\mathbf{U}^{i-1} + \alpha^{i-1} \Delta \mathbf{U}_e^i) \} \tag{16}$$

As with the original Thomas method, the procedure is started by assuming $\alpha^0 = 1$ during the first iteration of each load increment. After the displacements have been updated using Equation (15), the acceleration factor for the next iteration, α^i, is found by performing a least-squares fit so that

$$\alpha^i \Delta \mathbf{U}_e^i \approx \alpha^{i-1} \Delta \mathbf{U}_e^i + \Delta \tilde{\mathbf{U}}_e^i$$

This leads to the modified acceleration factor

$$\alpha^i = \alpha^{i-1} + \frac{\{\Delta \mathbf{U}_e^i\}^T \{\Delta \tilde{\mathbf{U}}_e^i\}}{\{\Delta \mathbf{U}_e^i\}^T \{\Delta \mathbf{U}_e^i\}} \tag{17}$$

This algorithm, which we will refer to as the modified Thomas scheme, needs two backsubstitutions and two unbalanced force evaluations for each iteration. Both forms of the Thomas scheme have proved to be very robust when applied to large-scale plasticity problems with complicated constitutive models. One possible explanation for this follows from the nature of the two terms used in the iterative displacement update. In Equation (15), the term $\alpha^{i-1} \Delta \mathbf{U}_e^i$ can be interpreted as being the 'dangerous', part of the update, since the accelerator α^{i-1} may often be quite large (in excess of 10). This component, however, tends to be 'stabilised', by the remaining term which uses the unbalanced forces at the displacements $\mathbf{U}^{i-1} + \alpha^{i-1} \Delta \mathbf{U}_e^i$ to compute the elastic displacements given by (16).

3. APPLICATIONS

In this section, the acceleration schemes described above are used to analyse the expansion of a thick cylinder, the collapse of a rigid strip footing, and the failure of a vertical cut. Each of these elastoplastic problems is modelled using either a cohesive-frictional Mohr–Coulomb yield surface, to simulate drained loading, or a purely cohesive Tresca yield criterion, to model undrained loading. Both of these yield criteria have been smoothed to eliminate all singularities in their gradients. The rounding procedures for the Tresca and Mohr–Coulomb surfaces are described, respectively, in Reference [15,16]. The Mohr–Coulomb smoothing scheme adopts a hyperbolic approximation in the meridional plane to remove the tip singularity, and a trigonometric approximation in the octahedral plane to remove the corner singularities, and requires only two parameters to fit the exact Mohr–Coulomb criterion as closely as desired. This approach removes the need to develop special constitutive integration procedures in the vicinity of the tip and corners, and is simple to implement.

At the stress point level, the elastoplastic constitutive laws are integrated using an explicit scheme with error control as described in Reference [16]. This scheme is a refined version of the algorithm originally published by Sloan [17], and uses an Euler-modified Euler pair with adaptive substepping to control the integration error in the stresses. Following Crisfield [7], the constitutive relationships are always integrated using incremental, rather than iterative, strains. This implies that the iterative stress states are found by integrating the constitutive law from the last converged equilibrium state, which is usually at the start of the current load increment. This approach avoids the complicated strain paths and spurious unloading that occurs when iterative strains are used, and has been found to improve the reliability of most iterative solution schemes. For the results presented in this paper, the constitutive laws are integrated accurately by using a relative local error tolerance of 10^{-3} for the stresses in conjunction with an absolute tolerance of 10^{-6} for drift from the yield surface.

For each of the solution schemes, the iterations are terminated once the unbalanced forces are small in comparison to the externally applied loads. This criterion may be written as

$$\|\mathbf{R}^i\|_2 \leqslant ITOL\|\mathbf{F}_{\text{ext}}\|_2 \tag{18}$$

where $\mathbf{F}_{\text{ext}}$ is the total applied force at the end of the current load increment and $ITOL$ is a user specified tolerance.

3.1. Thick cylinder

The expansion of a thick cylinder of Mohr–Coulomb material is a useful test problem for which Yu [18] has derived an analytical solution. The finite element mesh, shown in Figure 1, models the geometry of a plane strain cylinder using six-noded triangles and the behaviour of the soil is described by the rounded Mohr–Coulomb yield surface of Abbo [16] with an associated flow rule. Loading is applied to the cylinder by a prescribed pressure, p, at the inner surface and a total pressure of $p/c = 0.9808$ is imposed during the analysis. This represents 96.5 per cent of the analytic collapse pressure of $p/c = 1.017$ predicted by Yu [18].

Finite element results are presented for the initial stiffness algorithm, the conventional Newton–Raphson scheme, and the Chen [12], Thomas [11] and modified Thomas [14] acceleration methods. Each solution scheme is used with 10, 20 and 50 equal-sized increments to apply the

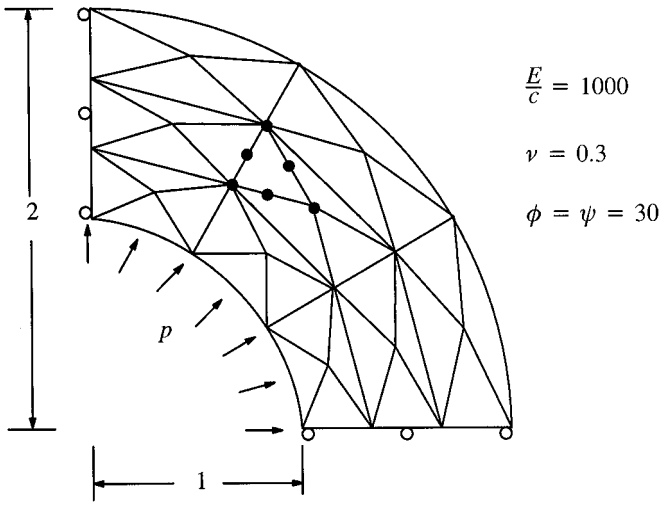

Figure 1. Thick cylinder, 36 elements, 142 degrees of freedom (E = Young's modulus, c = cohesion, ν = Poisson's ratio, ϕ = friction angle, ψ = dilation angle).

Table I. Results for thick cylinder of Mohr–Coulomb material ($E/c = 1000$, $\nu = 0.3$, $\phi = \psi = 30$, $p/c = 0.9808$).

Scheme	Total iterations			Normalized CPU time		
	10 inc.	20 inc.	50 inc.	10 inc.	20 inc.	50 inc.
Initial stiffness	507	684	1112	1.00	1.00	1.50
Chen	177	318	540	0.50	0.83	1.50
Thomas	91	148	285	0.67	0.83	1.83
Modified Thomas	101	162	283	0.33	0.50	0.67
Newton–Raphson	33	56	108	0.17	0.33	0.67

total pressure, and the number of iterations and CPU times are summarized in Table I. Note that the CPU times are normalized against the CPU time for the initial stiffness scheme with 10 increments. The simple nature of this problem enabled a stringent tolerance $ITOL = 10^{-8}$ to be specified in equation (18) to terminate the iteration process.

As expected, the initial stiffness scheme uses the most number of iterations taking 507, 684 and 1112 iterations for the runs with 10, 20 and 50 load increments, respectively. Of the acceleration methods, the Thomas and the modified Thomas schemes require the least number of iterations. They use 91 and 101 iterations, respectively, for the 10 increment analyses, 148 and 162 iterations for the 20 increment analyses and, 285 and 283 iterations for the analyses with 50 increments. This represents an average iteration reduction of approximately 79 per cent compared with the initial stiffness scheme. In comparison, the Chen scheme gives iteration savings of 65, 54 and 51 per cent. As a benchmark, the rapid convergence of the Newton–Raphson scheme reduces the number of iterations by an average of 92 per cent, requiring only 33, 56 and 108 iterations for the three analyses.

Table II. Iteration counts for 10-increment analyses of thick cylinder of Mohr–Coulomb material ($E/c = 1000$, $v = 0.3$, $\phi = \psi = 30$, $p/c = 0.9808$).

Increment No.	Initial stiffness	Chen	Thomas	Modified Thomas	Newton–Raphson
1 to 6	6	6	6	6	6
7	40	21	11	11	5
8	69	38	14	15	7
9	94	44	19	19	7
10	298	68	41	50	8
Total	507	177	91	101	33

A better indication of the performance of the various solution strategies is their total CPU time, as this reflects their computational complexity. The fastest acceleration method is the modified Thomas scheme which, compared with the equivalent initial stiffness analysis, yields CPU time reductions of 67, 50 and 55 per cent for the runs with 10, 20 and 50 load increments, respectively. Not surprisingly, the largest savings occur for the analysis with the coarsest load increments, where the effect of acceleration is greatest. The CPU time savings are largest for the Newton–Raphson scheme, and range from 83 per cent for the 10 increment analysis to 55 per cent for the 50 increment analysis. Interestingly, for the 50 increment run, the modified Thomas scheme is just as efficient as the Newton–Raphson method. The differences in CPU time between the Thomas and modified Thomas methods is largely due to the replacement of the product $\mathbf{K}_p\Delta\mathbf{U}^k$ by the residual $\mathbf{R}(\mathbf{U}^k + \alpha^{k-1}\Delta\mathbf{U}^k)$ when the displacement update is computed. For small load steps, we expect the iteration counts for these two methods to be very similar, as observed, but it is generally faster to evaluate the residual than to evaluate the matrix-vector product. Compared to the modified Thomas scheme, the Chen scheme is not competitive for this example.

The numbers of iterations required in each increment of the 10 increment analyses are shown in Table II. All the schemes require only a single iteration in each of the first six increments due to the fact that the behaviour is elastic. For the remaining increments, the number of iterations grows in line with the spread of plasticity throughout the cylinder. Near collapse, the Newton–Raphson scheme requires fewer iterations than the initial stiffness and accelerated initial stiffness schemes.

Finally, the load–displacement response for the runs with 10 increments is shown in Figure 2 (all analyses give essentially the same response for the scale used). Allowing for discretization effects, the finite element results agree well with the analytic solution given by Yu [18].

3.2. Rigid strip footing on Tresca material

We now consider the problem of a smooth rigid strip footing resting on a weightless purely cohesive soil. Due to the singularity at the edge of the footing and the strong rotation of the principal stresses, this case is a severe test for non-linear solution schemes. The finite element mesh and boundary conditions used are shown in Figure 3. Vertical load is applied to the footing by a set of uniform prescribed displacements. An equivalent pressure, p, is computed by summing the appropriate nodal reactions and dividing by the footing area. A total of 48 cubic strain triangles is used in the grid, and these are concentrated under the edge of the footing in an effort to

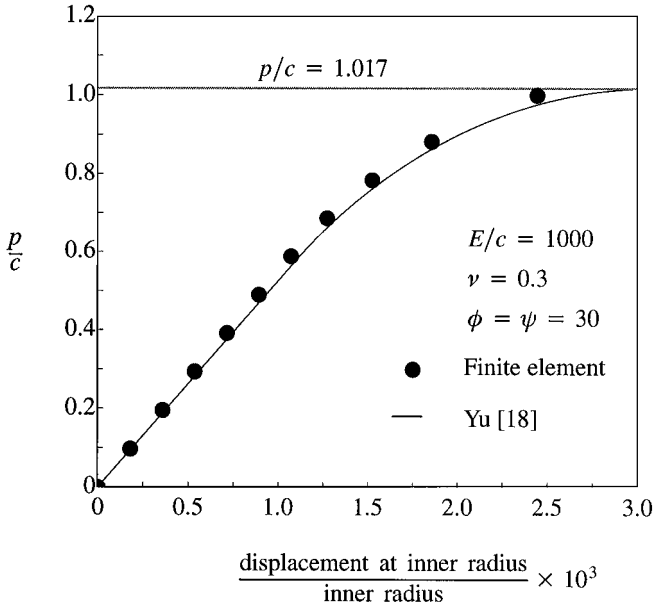

Figure 2. Load vs displacement for cylinder expansion in Mohr–Coulomb material with associated flow rule.

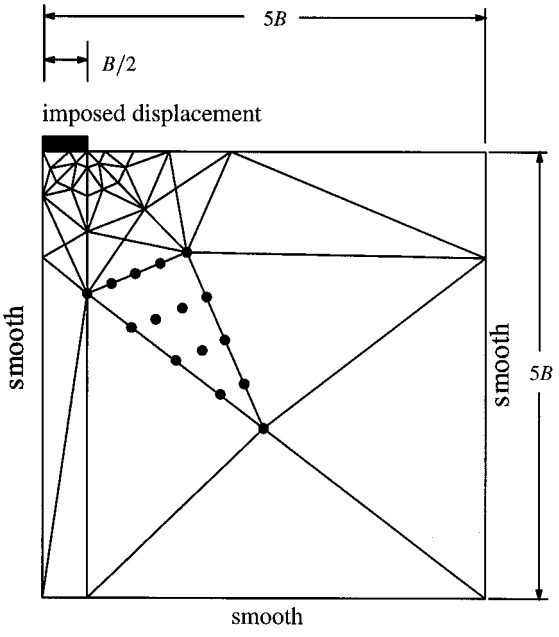

Figure 3. Rigid strip footing on elastoplastic soil (48 elements, 786 degrees of freedom).

Table III. Results for strip footing on Tresca material ($E/c = 298$, $v = 0.3$, footing displacement/$B = 0.11$).

Scheme	Total iterations			Normalized CPU time		
	10 inc.	20 inc.	50 inc.	10 inc.	20 inc.	50 inc.
Initial stiffness	377	448	600	1.00	0.85	0.88
Chen	190	247	374	0.98	0.88	0.98
Thomas	140	177	251	1.15	1.32	1.73
Modified Thomas	96	139	239	0.54	0.56	0.73
Newton–Raphson	58	58	78	0.41	0.39	0.49

model the singularity. These elements are known to avoid locking for incompressible materials and also give accurate predictions for dilatational plasticity models (see [19,20]). As for the thick cylinder, the footing is analysed using 10, 20 and 50 equal-size load increments with each of the acceleration schemes. A convergence tolerance of $ITOL = 10^{-3}$ is employed for all runs and the rounded Tresca yield criterion is used with the following material parameters:

$$E/c = 298, \quad v = 0.499$$

The results of these analyses, for a total footing displacement of $0.11B$ (which is sufficient to cause plastic collapse), are presented in Table III.

For this example, the modified Thomas scheme is again the most effective acceleration scheme. Compared with the initial stiffness algorithm, it yields CPU time savings of 46, 34 and 17 per cent for the 10, 20 and 50 increment runs, respectively. The largest savings again occur for the case with the coarsest load steps. The original Thomas scheme, although giving significant iteration reductions, is less efficient in terms of CPU time. Indeed, for all the examples analysed, it uses more CPU time than the initial stiffness method. For the analyses with smaller load steps, the iteration counts for the original Thomas scheme approach those of the modified Thomas scheme, but the cost of forming $\mathbf{K}_p\Delta\mathbf{U}^k$ for each iteration is clearly high. Similarly, the Chen acceleration scheme provides significant iteration reductions but is not computationally competitive. As in the previous example, the Newton–Raphson algorithm requires the fewest iterations, with iteration counts that are about 87 per cent lower than the initial stiffness method. On average, the Newton–Raphson scheme is 29 per cent faster than the modified Thomas scheme.

The numbers of iterations used in each step of the 10 increment Tresca footing analyses are listed in Table IV. Because of the displacement controlled loading, the number of iterations at incipient collapse for this case is lower than that for the thick cylinder. Although load–deformation plots are not shown, all of the methods estimated the exact collapse load of $p/c = 2 + \pi$ to within 2 per cent.

Many practical finite element calculations do not require the structure to be loaded to the point of collapse. Indeed, the response under working loads is often of more interest. To investigate the performance of the various schemes under typical working load deformations, the footing case just considered was reanalysed with a total imposed footing displacement of $0.055B$, which is half the displacement needed to cause collapse. The results shown in Table V indicate that, in terms of CPU time, the initial stiffness method is much more competitive with the Newton–Raphson and modified Thomas algorithms. Indeed, for the analysis with 50 load steps, the initial stiffness

Table IV. Iteration counts for 10-increment analyses of strip footing on Tresca material ($E/c = 298$, $v = 0.3$, footing displacement/$B = 0.11$).

Increment No.	Initial stiffness	Chen	Thomas	Modified Thomas	Newton–Raphson
1	7	5	5	4	4
2	19	12	9	7	6
3	45	21	15	11	10
4	42	22	13	11	6
5	45	24	19	11	4
6	43	19	16	10	5
7	41	20	14	10	5
8	42	21	14	10	6
9	45	24	15	11	6
10	48	22	20	11	6
Total	377	190	140	96	58

Table V. Results for strip footing on Tresca material under working load ($E/c = 298$, $v = 0.3$, footing displacement/$B = 0.055$).

Scheme	Total iterations			Normalized CPU time		
	10 inc.	20 inc.	50 inc.	10 inc.	20 inc.	50 inc.
Initial stiffness	198	249	347	1.00	1.07	1.29
Chen	108	159	250	1.00	1.14	1.57
Thomas	78	106	164	1.57	2.07	3.00
Modified Thomas	63	97	163	0.71	0.86	1.14
Newton–Raphson	34	42	79	0.57	0.71	1.36

scheme is marginally faster than the former and only 13 per cent slower than the latter. On average, the initial stiffness and modified Thomas algorithms are, respectively, 40 and 10 per cent slower than the Newton–Raphson procedure.

3.3. Rigid strip footing on associated Mohr–Coulomb material

We now consider the same problem as shown in Figure 3, but with the footing resting on a Mohr–Coulomb material. In these analyses, the dilation angle ψ is assumed to equal the friction angle ϕ, implying an associated flow rule, and the following material parameters are adopted:

$$E/c = 1040, \quad v = 0.3, \quad \phi = \psi = 30 \tag{19}$$

A uniform displacement equal to $0.16B$ is imposed on the footing, which is sufficient to invoke collapse. The load displacement plot for the 10 increment analyses, shown in Figure 4, captures the exact Prandtl collapse load of $p/c = 30.14$ to within 3 per cent. The iteration counts and CPU times, summarized in Table VI, indicate that the modified Thomas scheme is again the most

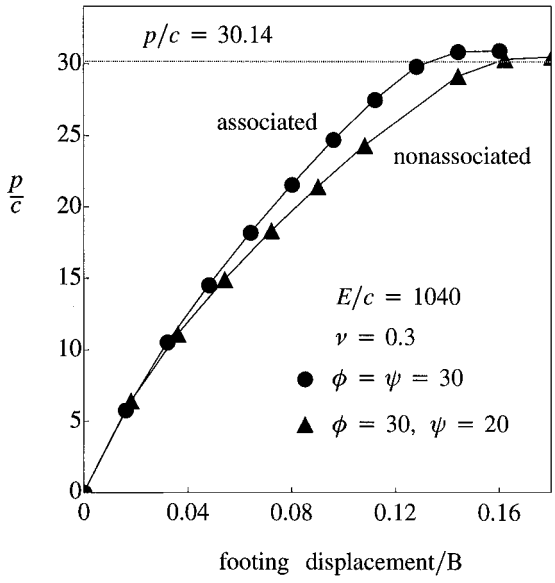

Figure 4. Load versus displacement for rigid footing on Mohr–Coulomb material.

Table VI. Results for strip footing on Mohr–Coulomb material ($E/c = 1040$, $\nu = 0.3$, $\phi = \psi = 30$, footing displacement/$B = 0.16$).

Scheme	Total iterations			Normalized CPU time		
	10 inc.	20 inc.	50 inc.	10 inc.	20 inc.	50 inc.
Initial stiffness	2125	2768	3675	1.00	0.80	0.72
Chen	561	725	1057	0.45	0.39	0.36
Thomas	377	449	688	0.39	0.39	0.53
Modified Thomas	314	455	656	0.37	0.29	0.28
Newton–Raphson	76	79	98	0.07	0.06	0.07

efficient acceleration algorithm. Compared with the initial stiffness method, it yields average iteration and CPU time savings of 84 and 63 per cent, respectively. The percentage CPU time reductions for the original Thomas scheme range from 61 to 26 percent, with the largest savings occurring for runs with coarse load steps. Compared to the modified Thomas scheme, the Chen scheme requires 79–61 per cent more iterations, and is less efficient for the runs with large load steps. By the far the most effective solution strategy for this problem, however, is the Newton–Raphson scheme which, compared with the initial stiffness method, gives an average CPU time saving of around 92 per cent. Compared with the modified Thomas method, the Newton–Raphson scheme is faster by an average factor of 4.5. Iteration counts for the various 10 increment analyses, shown in Table VII, indicate that the Newton–Raphson method typically uses a quarter of the iterations needed for the modified Thomas method over the entire loading

Table VII. Iteration counts for 10-increment analyses of strip footing on Mohr–Coulomb material ($E/c = 1040$, $v = 0.3$, $\phi = \psi = 30$, footing displacement/$B = 0.16$).

Increment No.	Initial stiffness	Chen	Thomas	Modified Thomas	Newton–Raphson
1	54	17	11	10	7
2	181	37	46	27	11
3	176	45	44	27	8
4	155	75	37	24	7
5	156	46	35	23	6
6	169	45	35	25	6
7	181	38	31	27	5
8	214	42	38	38	6
9	305	95	39	55	7
10	534	121	61	58	13
Total	2125	561	377	314	76

Table VIII. Results for strip footing on Mohr–Coulomb material under working load ($E/c = 1040$, $v = 0.3$, $\phi = \psi = 30$, footing displacement/$B = 0.08$).

Scheme	Total iterations			Normalized CPU time		
	10 inc.	20 inc.	50 inc.	10 inc.	20 inc.	50 inc.
Initial stiffness	951	1302	1876	1.00	1.03	1.23
Chen	293	400	589	0.57	0.58	0.68
Thomas	185	263	430	0.65	0.85	1.33
Modified Thomas	175	244	422	0.36	0.39	0.55
Newton–Raphson	40	49	86	0.14	0.15	0.24

range. This saving clearly offsets the additional cost of forming the tangent stiffness matrix for each iteration.

Table VIII summarizes various results for a total imposed footing displacement of $0.08B$, which is roughly half the collapse value and corresponds to a typical working load. Under this loading, the performance of the modified Thomas scheme is more competitive with the Newton–Raphson technique but is still slower by a factor of around 2.5. Compared with the initial stiffness method, the modified Thomas procedure gives an average speed-up of 60 per cent, while the Newton scheme gives an average speed-up of 84 per cent. The Chen scheme is less effective than the modified Thomas method and the original Thomas algorithm is inefficient in terms of CPU time for runs with small load increments.

3.4. Rigid footing on non-associated Mohr–Coulomb material

So far, all the analyses have used associated flow rules. In this section, we investigate the performance of the various solution schemes for a rigid footing resting on a Mohr–Coulomb

Table IX. Results for strip footing on non-associated Mohr–Coulomb material ($E/c = 1040$, $v = 0.3$, $\phi = 30$, $\psi = 20$, footing displacement/$B = 0.18$).

Scheme	Total iterations			Normalized CPU time		
	10 inc.	20 inc.	50 inc.	10 inc.	20 inc.	50 inc.
Initial stiffness	2749	3366	4509	1.00	0.77	0.65
Chen	687	907	1912	0.45	0.33	0.30
Thomas	461	507	799	0.37	0.34	0.48
Modified Thomas	391	535	760	0.32	0.25	0.27
Newton–Raphson	87	82	97	0.08	0.06	0.07

material with a nonassociated flow rule. This type of model is different to the previous case because it gives rise to an unsymmetric stiffness matrix so that an unsymmetric equation solver must be used for the Newton–Raphson method. The mesh shown in Figure 3 is again employed for the analyses and the material properties adopted are

$$E/c = 1040, \quad v = 0.3, \quad \phi = 30, \quad \psi = 20 \tag{20}$$

In the first set of runs, a displacement of $0.18B$, which is sufficient to cause collapse, is imposed on the footing. The results for these analyses, presented in Table IX, indicate that all the acceleration schemes give large reductions in the number of iterations when compared with the initial stiffness method. The modified Thomas method, for example, reduces the iterations by an average factor of 6.4, while the Chen scheme gives a reduction factor of around 3.4.

Interestingly, the Newton–Raphson algorithm is still the fastest method, despite the fact that the tangent stiffness matrix is now unsymmetric and takes twice as much effort to form and factorise. Compared with the initial stiffness scheme, it gives average CPU time reductions of 93 per cent and is typically four times faster than the modified Thomas algorithm. Although the Chen scheme is less effective than the Thomas methods in reducing the number of iterations, its performance in reducing CPU time is close to that of the modified Thomas algorithm for runs with small load increments. The iteration counts for the various 10 increment analyses, shown in Table X, indicate that the Newton–Raphson scheme is more efficient because it does not use excessive numbers of iterations approaching collapse.

The load deformation plots for the various 10 increment analyses with a non-associated flow rule, shown in Figure 4, suggest that the value of the collapse load is relatively insensitive to the value of the dilation angle. Indeed, the collapse loads for the associated and non-associated cases differ by less than 2 per cent for the case considered here. This characteristic has been observed elsewhere (see, for example, [21] or [22]) and is generally exhibited by problems which are not strongly constrained in a kinematic sense.

For a working load footing displacement of $0.09B$, the results shown in Table XI suggest that the Newton–Raphson scheme is still the fastest solution strategy, albeit by a smaller margin. On average, it is faster than the initial stiffness method by a factor of 5.2 and faster than the modified Thomas scheme by a factor of 1.9. As in previous Mohr–Coulomb runs, the speed advantage of the Newton–Raphson algorithm appears to be greatest for cases with the largest load steps, and diminishes slowly as the size of the load steps is reduced.

Table X. Iteration counts for 10-increment analyses of strip footing on non-associated Mohr–Coulomb material ($E/c = 1040$, $\nu = 0.3$, $\phi = 30$, $\psi = 20$, footing displacement/$B = 0.18$).

Increment No.	Initial stiffness	Chen	Thomas	Modified Thomas	Newton–Raphson
1	64	20	13	11	9
2	209	66	55	34	11
3	181	51	46	27	9
4	164	38	40	25	7
5	175	58	40	26	7
6	188	50	36	27	6
7	222	43	39	38	6
8	322	76	39	56	8
9	592	133	76	72	14
10	632	152	77	75	10
Total	2749	687	461	391	87

Table XI. Results for strip footing on non-associated Mohr–Coulomb material under working load ($E/c = 1040$, $\nu = 0.3$, $\phi = 30$, $\psi = 20$, footing displacement/$B = 0.09$).

Scheme	Total iterations			Normalized CPU time		
	10 inc.	20 inc.	50 inc.	10 inc.	20 inc.	50 inc.
Initial stiffness	1036	1402	2022	1.00	1.01	1.17
Chen	343	427	618	0.61	0.55	0.61
Thomas	203	266	446	0.69	0.83	1.32
Modified Thomas	179	259	440	0.34	0.36	0.50
Newton–Raphson	42	52	86	0.16	0.18	0.30

3.5. Vertical cut in Tresca material

The final problem to be considered is the undrained failure of a vertical cut in a Tresca material. The geometry, finite element mesh and material properties for this case are shown in Figure 5, where the cut is loaded by gradually increasing the unit weight γ. Although the exact collapse load for this problem is unknown, Pastor [23] has shown that it is strictly bounded by the dimensionless stability numbers $\gamma H/c = 3.64$ and $\gamma H/c = 3.83$. Figure 6 shows a plot of the applied unit weight versus maximum horizontal displacement (on the face of the cut) for a finite element analysis with 20 equal sized load increments. These results clearly indicate a state of collapse for $\gamma H/c = 4.1$, which is about 7 per cent over the best upper bound from classical limit analysis.

The results for the runs with 10, 20 and 50 increments in the unit weight, summarized in Table XII, suggest that the modified Thomas scheme is again the best of the acceleration schemes. Compared with the initial stiffness method, it typically gives a twofold reduction in the total number of iterations but similar overall CPU times. The latter observations is consistent with the fact that the modified Thomas scheme involves roughly twice as much work per iteration as the initial stiffness method. The original Thomas scheme, although giving similar iteration counts to the modified Thomas scheme, is uncompetitive in terms of CPU time. Unlike previous examples,

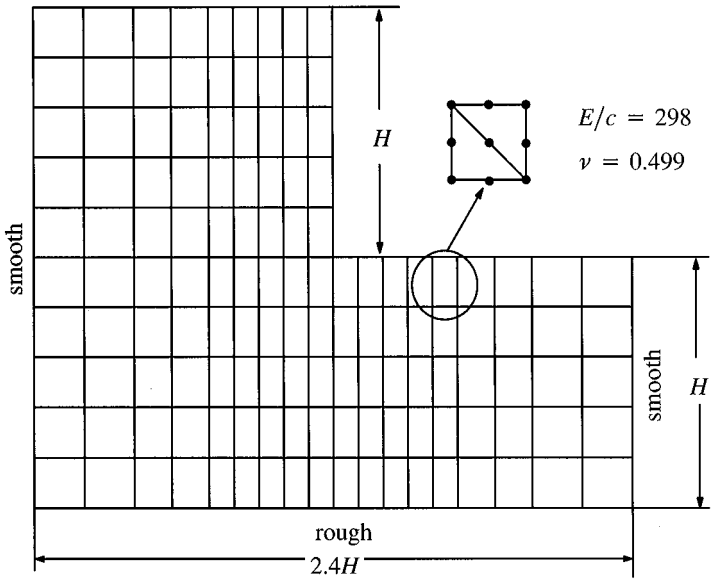

Figure 5. Vertical cut in Tresca material (270 elements, 986 degrees of freedom).

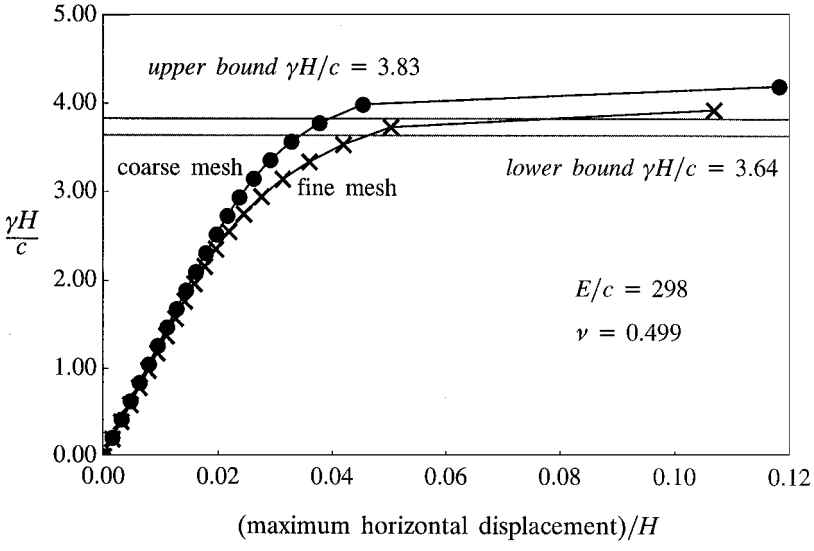

Figure 6. Unit weight versus maximum horizontal displacement for vertical cut in Tresca material.

the Newton–Raphson algorithm is no longer the method of choice and, on average, is slower than the modified Thomas method by a factor of 2.5. For this problem the Chen accelerator is quite competitive, being only marginally slower than the modified Thomas scheme.

Table XII. Results for vertical cut in Tresca material ($E/c = 298$, $\nu = 0.499$, $\gamma H/c = 4.1$, DOF = 986).

Scheme	Total iterations			Normalized CPU time		
	10 inc.	20 inc.	50 inc.	10 inc.	20 inc.	50 inc.
Initial stiffness	70	97	151	1.00	1.33	1.67
Chen	41	59	103	1.00	1.33	1.67
Thomas	41	47	87	4.33	4.67	8.33
Modified Thomas	28	45	83	0.67	1.33	1.67
Newton–Raphson	29	39	64	2.00	2.67	4.33

Table XIII. Iteration counts for 10-increment analyses of vertical cut in Tresca material ($E/c = 298$, $\nu = 0.499$, $\gamma H/c = 4.1$, DOF = 986).

Increment No.	Initial stiffness	Chen	Thomas	Modified Thomas	Newton–Raphson
1	1	1	1	1	1
2	1	1	1	1	1
3	1	1	1	1	1
4	4	2	3	2	2
5	4	3	2	2	2
6	5	4	3	3	2
7	6	4	3	3	2
8	7	4	3	3	3
9	11	6	4	4	3
10	30	15	20	8	12
Total	70	42	41	28	29

The iteration counts for the various 10 increment runs, shown in Table XIII, suggest that the modified Thomas method is very effective at limiting the number of iterations over the entire loading range. Moreover, it requires the smallest number of iterations in the last load increment, where the cut is clearly undergoing extensive shear failure.

To examine the effect of increasing the number of degrees of freedom (DOF), the vertical cut problem was analysed again using the same material properties but a much finer mesh. The refined grid, shown in Figure 7, has 2742 degrees of freedom, which is almost a threefold increase on the degrees of freedom used for the mesh of Figure 5. For this fine mesh, collapse occurs at the slightly lower value of $\gamma H/c = 3.93$ (see Figure 6). The iteration counts, summarized in Table XIV, are very similar to those obtained for the coarse mesh and typically differ by less than 1 or 2 iterations. The CPU times in this table also display similar patterns to those in Table XII, with the modified Thomas and Chen acceleration procedures being the fastest and the Thomas accelerator being the slowest. The initial stiffness method is again one of the most efficient solution methods for this example. The Newton–Raphson scheme is slower than the modified Thomas scheme by a factor of around 3.6, and is thus uncompetitive. The iteration counts and the

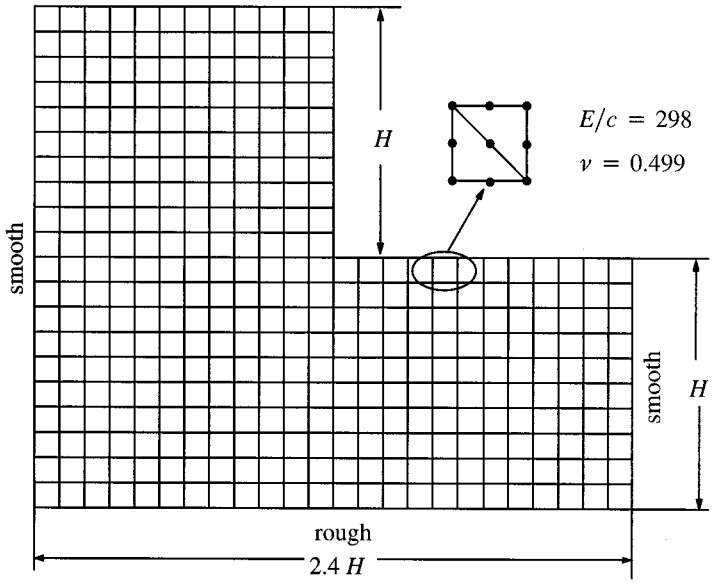

Figure 7. Vertical cut in Tresca material (720 elements, 2742 degrees of freedom).

Table XIV. Results for vertical cut in Tresca material ($E/c = 298$, $\nu = 0.499$, $\gamma H/c = 3.93$, DOF = 2742).

Scheme	Total iterations			Normalized CPU time		
	10 inc.	20 inc.	50 inc.	10 inc.	20 inc.	50 inc.
Initial stiffness	72	99	150	1.00	1.20	1.70
Chen	41	61	103	0.90	1.10	1.50
Thomas	30	48	82	4.30	6.50	10.8
Modified Thomas	29	47	82	0.80	1.10	1.80
Newton–Raphson	27	40	62	2.90	4.20	6.30

CPU times shown in Table XIII and XIV indicate that the number of degrees of freedom does not, for this case, significantly alter the performance rankings of the various solution schemes.

4. CONCLUSIONS

A variety of numerical experiments were conducted to compare the performance of single-parameter, initial stiffness acceleration schemes. These analyses used the Tresca and Mohr–Coulomb yield criteria which are common in soil mechanics. Although most of the acceleration schemes studied significantly improved the performance of the initial stiffness scheme, the modified Thomas algorithm would appear to be the method of choice on the basis of the data presented here. Averaging over all the problems considered, it gives a 74 per cent

reduction in iterations and a 45 per cent reduction in CPU time and has proved very robust for large-scale plasticity computations. The original Thomas method gives similar iteration reductions, but is much less efficient if the matrix-vector product $\mathbf{K}_p\Delta\mathbf{U}_e^i$ is evaluated element by element in Equation (11). In general, the Chen scheme is not competitive with the modified Thomas scheme, even though it does give substantial CPU time reductions for some problems.

Although the modified Thomas method is less efficient than the Newton–Raphson algorithm for cohesive-frictional materials, either with or without an associated flow rule, it is certainly competitive for undrained problems which use the Tresca criterion. It is also competitive for cases where the spread of plasticity is limited, such as under working load conditions.

All of the acceleration schemes discussed in this paper can be generalized to cater for more complex constitutive models which incorporate both hardening and softening. With the latter type of behaviour, of course, appropriate steps must be taken to ensure that the solution is objective at the global level. For models with nonlinear elastic behaviour inside the yield surface, such as those based on critical state principles, the definition of the elastic stiffness matrix becomes vague. In these cases, it is possible to apply the accelerators to a modified Newton–Raphson iteration where the elastic stiffness is replaced by the stiffness at the start of the current load increment. For the sake of simplicity and clarity, these types of models have not been included in the present study.

REFERENCES

1. Matthies H, Strang G. The solution of non-linear finite element equations. *International Journal for Numerical Methods in Engineering* 1979; **14**:1613–1626.
2. Crisfield MA. An arc-length method including line searches and accelerations. *International Journal for Numerical Methods in Engineering* 1983; **19**:1269–1289.
3. Crisfield MA. Accelerating and damping the modified Newon–Raphson method. *Computers and Structures* 1984; **18**: 395–407.
4. Wempner GA. Discrete approximations related to nonlinear theories of solids. *International Journal of Solids and Structures* 1971; **7**:1581–1599.
5. Riks E. The application of Newtons method to the problem of elastic instability. *Journal of Applied Mechanics* 1972; **39**:1060–1066.
6. Riks E. An incremental approach to the solution of snapping and buckling problems. *International Journal of Solids and Structures* 1979; **15**: 529–551.
7. Crisfield MA. *Non-linear Finite Element Analysis of Solids and Structures*, vol. 1. Wiley: Chichester, 1991.
8. Simo JC, Taylor RL. Consistent tangent operators for rate-independent elastoplasticity. *Computer Methods in Applied Mechanics and Engineering* 1985; **48**:101–118.
9. Nayak GC, Zienkiewicz OC. Elasto-plastic stress analysis. A generalisation for various constitutive relations including strain softening. *International Journal for Numerical Methods in Engineering* 1972; **5**:113–135.
10. Nayak GC, Zienkiewicz OC. Note on the 'alpha'—constant stiffness method for the analysis of non-linear problems. *International Journal for Numerical Methods in Engineering* 1972; **4**:579–582.
11. Thomas JN. An improved accelerated initial stress procedure for elasto-plastic finite element analysis. *International Journal for Numerical and Analytical Methods in Geomechanics* 1984; **8**:359–379.
12. Chen C. Efficient and reliable accelerated constant stiffness algorithms for the solution of non-linear problems. *International Journal for Numerical Methods in Engineering* 1992; **35**:481–490.
13. Liu L, Lam YC. Acceleration procedures for non-linear finite element analysis based on an energy criterion. *Proceedings of the 2nd Asian-Pacific conference on Computational Mechanics*, vol. 2, Sydney, Australia, 1993; 1325–1329.
14. Abbo AJ, Sloan SW. Accelerated initial stiffness schemes for elastoplasticity. In *Computational Plasticity*, *Proceedings of 5th International conference*, Owen DRJ, Onate O, Hinton E. (eds), vol. 2. International Center for Numerical Methods in Engineering: Barcelona, Spain, 1997; 334–342.
15. Sloan SW, Booker JR. Removal of singularities in Tresca and Mohr–Coulomb yield functions. *Communications in Applied Numerical Methods* 1986; **2**:173–179.

16. Abbo AJ. Finite element algorithms for elastoplasticity and consolidation. *Ph.D. Thesis. University of Newcastle, Australia*, 1997.
17. Sloan SW. Substepping schemes for the numerical integration of elastoplastic stress–strain relations. *International Journal for Numerical Methods in Engineering* 1987; **24**:893–911.
18. Yu HS. Expansion of a thick cylinder of soils. *Computers and Geotechnics* 1992; **14**:21–41.
19. Sloan SW, Randolph MF. Numerical prediction of collapse loads using finite element methods. *International Journal for Numerical and Analytical Methods in Geomechanics* 1982; **33**:163–196.
20. Sloan SW. *Numerical Analysis of incompressible and plastic solids using finite elements. Ph.D. Thesis*, University of Cambridge, 1981.
21. Zienkiewicz OC, Humpheson C, Lewis RW. Associated and nonassociated viscoplasticity and plasticity in soil mechanics. *Geotechnique* 1975; **25**:671–689.
22. Davis EH. Theories of plasticity of soil masses. In *Soil Mechanics Selected Topics*, Lee IK (ed.). Butterworths: London, 1968, 341–380.
23. Pastor J. Analyse limite: limite: determination de solutions statiques complètes. Applications au talus vertical. *Journal de Mechanique Appliquée* 1978; **2**:167–196.

